An algorithm for generating rock fracture patterns: mathematical analysis

Riley, Michael

DOI:
10.1023/B:MATG.0000039541.36356.61

Document Version
Publisher's PDF, also known as Version of record

Citation for published version (Harvard):
Riley, M 2004, 'An algorithm for generating rock fracture patterns: mathematical analysis', *Mathematical Geology*, vol. 36, no. 6, pp. 683-702. https://doi.org/10.1023/B:MATG.0000039541.36356.61

Mathematical Geology, Vol. 36, No. 6, August 2004 (© 2004)

An Algorithm for Generating Rock Fracture Patterns: Mathematical Analysis[1]

Michael S. Riley[2]

A statistical, rule-based algorithm for generating fracture patterns similar to those observed in Limestone is presented. For each fracture set, initial seed points are randomly positioned within the modelled domain with the same density as the fractures observed in the field. An orientation is associated with each point by sampling from the distribution of orientations for the corresponding fracture set. Fractures are then allowed to grow from the seed points in both directions with this orientation until they meet other fractures whereupon they continue or terminate according to a fixed probability. A mathematical analysis of this method is presented for the case in which fractures within a set are assumed to be parallel. Approximations to the distribution of semi-trace lengths are derived which are shown to be in good agreement with simulation results. Fracture spacing distributions are also derived for this case.

KEY WORDS: limestone, stochastic simulation, trace length, fracture spacing.

INTRODUCTION

Stochastic models of flow and transport in fractured rock, used regularly in hydrogeological, nuclear waste disposal and oil reservoir investigations, require realizations of fracture distributions based upon statistics gathered from field investigations and desk studies. The methods used to generate these distributions depend upon the style of fracturing observed in the host rock. This paper concentrates on the simulation of the type of fracturing seen in layered, sedimentary sequences, such as those forming the Lincolnshire Limestone aquifer in the United Kingdom. Part of this aquifer, which was chosen as the site for investigations into contaminant transport in dual-porosity rock (Riley, Ward, and Greswell, 2001), is charazterised by extensive, subhorizontal, bedding plane fissures separating strata containing subvertical fractures and fissures. Lloyd and others (1996) present fracture maps obtained from adjacent strata covering the same 10×8 m horizontal area (Fig. 1).

[1]Received 18 September 2002; accepted 20 February 2004.

[2]Hydrogeology Research Group, Earth Sciences, School of Geography, Earth and Environmental Sciences, University of Birmingham, Edgbaston, Birmingham B15 2TT, United Kingdom; e-mail: m.riley@bham.ac.uk

Three features of the maps are worthy of note. First, almost all fractures terminate at an intersection with another fracture, but not necessarily at the first one. Second, fracture sets, which can be identified quite clearly on the basis of orientation alone, appear to contain semi-regularly spaced fractures. Finally, only one fracture set is present at both levels, and very few individual fractures persist vertically. A three-dimensional simulation of the formation can be achieved by generating bedding plane features based upon borehole logging data and then creating two-dimensional fracture patterns for each layer in the system to represent subvertical breaks in the rock.

Fracture network simulators range in style between those that generate fracture patterns purely stochastically and those based upon the mechanics of fracture propagation as described by Olsen (1993) and Renshaw and Pollard (1994). A common stochastic method is to position fracture centers in a generation region using a homogeneous Poisson process with mean based upon the fracture density, P_{20}, and then to complete each fracture by independently generating an orientation and fracture length from statistical distributions. This Boolean method can be extended to include correlations between orientation and length and to simulate more regular fracture spacing by imposing repulsion between the locations of the fracture centers. It can, however, only reproduce the termination characteristics of the patterns in Figure 1 by ignoring the hanging ends of fractures and hence biasing the simulated fracture length distribution. Stochastic tessellation methods, which produce blocks of rock, fail to simultaneously reproduce the observed persistent fractures and respect fracture trace length distributions. Simulators based upon the mechanics of fracture propagation remain computationally expensive for large-scale problems. More recently, in an attempt to produce more realistic fracture patterns, a number of stochastic simulators incorporating some form of rule-based fracture propagation have been developed such as those of Swaby and Rawnsley (1996), Gringarten, (1998), and Josnin and others (2002). Horgan and Young (2000) also adopt a rule-based approach to model cracking in drying soils.

Of the stochastic methods, only the purely Boolean approach produces a clearly defined relationship between simulated trace length and the fracture statistics upon which the generation process is based and, in general, the relationship between simulated fracture spacing and stochastic model parameters is not well understood. The distributions of fracture trace length and spacing in rule-based methods usually have to be determined by lengthy, multiple simulations.

The principal aim of this paper is to introduce a simple, rule-based, stochastic method of generating fracture patterns in two dimensions, and to present an analysis of the method that allows the distributions of simulated fracture length and spacing to be derived directly from the model parameters without the need to create multiple realizations of the fracture network. The analysis also allows the generation method to be critically appraised in a quantitative manner and may also

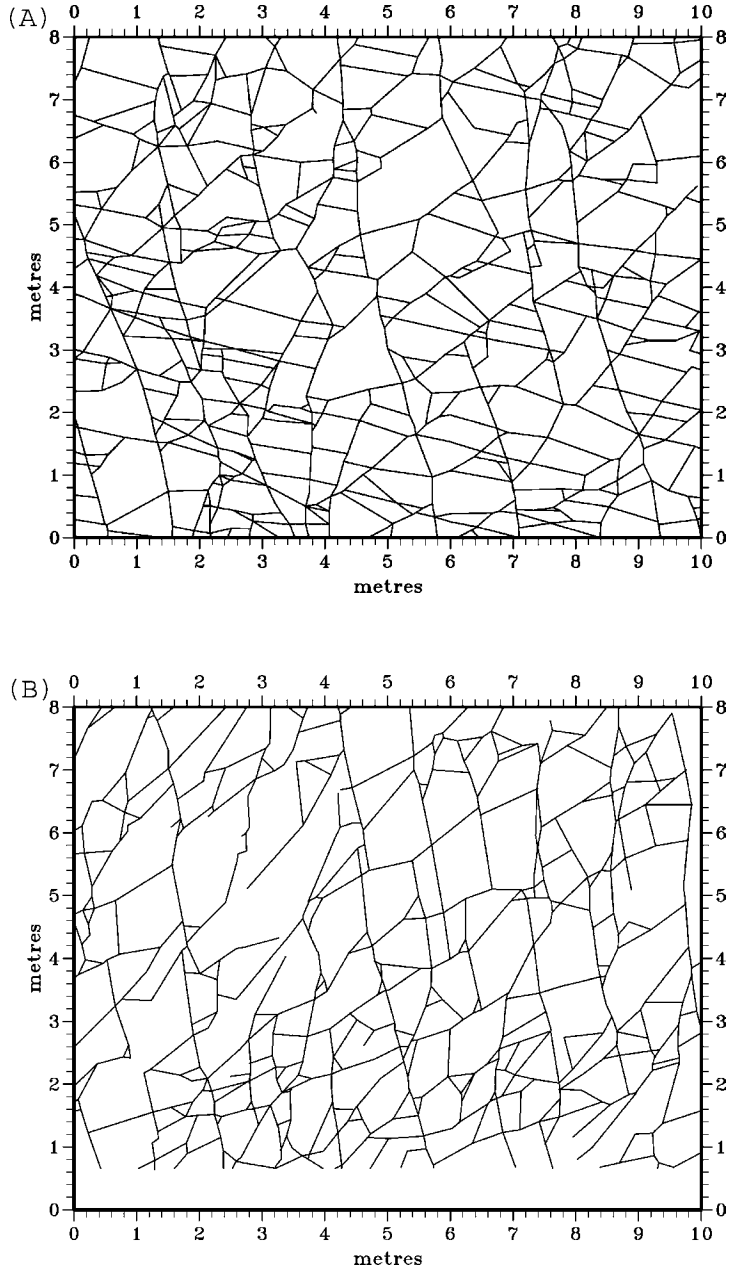

Figure 1. Maps showing the fractures in (A) the upper level and (B) the lower level beds at the experimental site. The upper bed is approximately 0.5 m thick.

provide insights into the behavior of similar techniques. The method analyzed in this paper is the simplest in a class of methods designed to simulate the style of fracturing seen in the Lincolnshire Limestone and similar layered rocks.

THE FRACTURE GROWTH ALGORITHM

The generation method proposed is based upon the propagation of cracks from a point of weakness in the rock. However, there has been no attempt to model the physics of crack propagation explicitly or to incorporate propagation velocity variations over time. It is assumed that, given time, all cracks terminate eventually at a preexisting fracture, but a growing crack may be allowed to cross existing fractures prior to termination. The algorithm proceeds as follows.

- For each fracture set, $i = 1, \ldots, n$, seed points are positioned within the modelled generation region with the same density, ρ_i, as that of the fractures observed in the field.
- An orientation is associated with each point by sampling the distribution of orientations determined from field data that relate to the fracture set in question.
- Each fracture is then allowed to grow from the seed point in both directions parallel to that orientation at speed, u_i, until it meets other fractures whereupon it continues according to a fixed probability, p_i.

PARALLEL FRACTURE MODEL

The variants on this method within the above structure are numerous. However, the simplest version of the growth algorithm constitutes a special case in which fracture density within a set is homogeneous, all fractures in a set are parallel, the speed of propagation is constant and the same for each fracture in a set, and all fractures are initiated simultaneously. An example of a fracture pattern generated using this version is shown in Figure 2.

This parallel fracture model has four parameters for each fracture set. The fracture density and the fracture orientation can be determined from field data and are reproduced automatically by the method. The parameters u_i and p_i are used to match the statistical distributions of fracture trace lengths produced by the method with those determined from field observations. A mathematical analysis of this variant of the method is outlined below.

MATHEMATICAL ANALYSIS

For fractures from set i, consider the distance from the seed point of a fracture to one of its ends to be represented by the random variable, X_i, which is

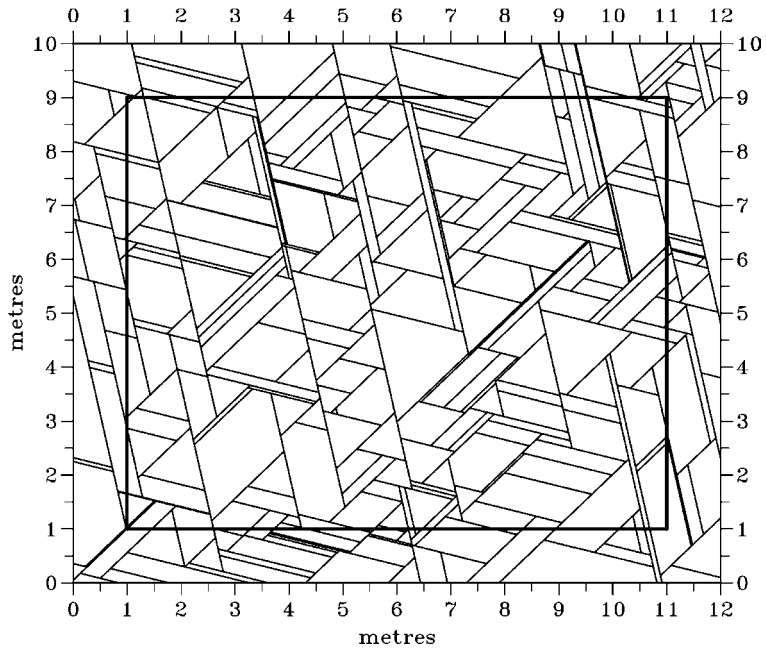

Figure 2. A single fracture pattern realization produced by the base case growth algorithm using an arbitrary parameter set. A 1 m guard zone has been introduced around the model area to minimize edge effects.

charazterised by its cumulative distribution function, $F_i(x)$. If the fracture densities are homogeneous in space, the total trace length of a fracture can then be considered as the sum of two independently drawn samples from $F_i(x)$, and so if $F_i(x)$ is known, the cumulative distribution function and the probability density function of the full trace length can, in principle, be determined. In this section approximations to $F_i(x)$ are derived in terms of the parameters of the generation algorithm.

For ease of exposition, consider first the case in which there are just two fracture sets, i and j. Figure 3 shows a fracture from set i growing from the point O in the direction OP with speed u_i. Displacement from O along OP is x and the growing tip of the fracture at any time is at $x = \xi$. This fracture grows until it meets a preexisting fracture from set j whereupon it continues growing or terminates according to the fixed probability p_i. Figure 3 also shows a fracture from set j growing from Q with speed u_j towards OP. The distance from its seed point to OP, measured along its length, is r. The angle between the fracture sets is θ_{ij}.

For the case of two fracture sets, it is convenient to add a second subscript, j, to $F_i(x)$ to emphasize that there is only one other set, j, under consideration. To calculate $F_{ij}(x)$, it is necessary to know how many intersections with preexisting

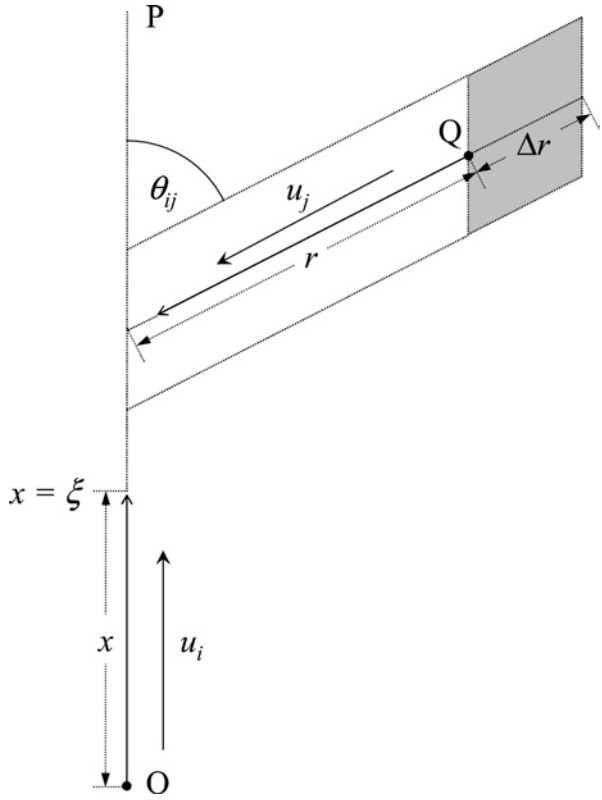

Figure 3. A fracture from set *i* grows from the point O in the direction OP and may be intercepted by another growing fracture from set j.

fractures occur, on average, within a given time t. This is a function of $F_{ji}(r)$, the cdf of the distance from the point at which a fracture from set j is seeded to its end. But, of course, to determine $F_{ji}(r)$, it is necessary to know how many intersections there are likely to be at time t between fractures from set j with preexisting fractures from set i and this is a function of $F_{ij}(x)$. The approach adopted is to obtain an expression for $F_{ij}(x)$ in terms of $F_{ji}(r)$ and then by similar argument to show how a closed, implicit expression for $F_{ij}(x)$ can be developed by deriving $F_{ji}(r)$ in terms of $F_{ij}(x)$.

To start, let $\lambda_{ij}(\xi)$ be the density (per unit length of OP) of fractures from set j intersecting the line OP at $x = \xi$. Then the expected number of fractures from set j intersecting the segment of length x starting from O is given by

$$g_{ij}(x) = \int_0^x \lambda_{ij}(\xi)\, d\xi \tag{1}$$

It is assumed that the number of intersections can be modelled by a Poisson process with nonhomogeneous mean, $g_{ij}(x)$. Thus, if $X_i(n)$ is the distance from O to the nth encounter, then

$$P(X_i(n) \leq x) = 1 - \exp[-g_{ij}(x)] \sum_{k=0}^{n-1} \frac{[g_{ij}(x)]^k}{k!} \tag{2}$$

Let p_i be the constant probability that a fracture from set i continues after encountering another fracture, and let N be the number of encounters from O to the end of the fracture. Then the probability that the growing fracture terminates at the nth encounter is given by

$$P(N = n) = p_i^{n-1}(1 - p_i) \tag{3}$$

Since X_i is the distance from the origin of the fracture to its end, the distribution function of X_i is given by

$$\begin{aligned} F_{ij}(x) &= P(X_i \leq x) \\ &= \sum_{n=1}^{\infty} P(X_i(n) \leq x \text{ and } N = n) \\ &= \sum_{n=1}^{\infty} \left\{ 1 - \exp[-g_{ij}(x)] \sum_{k=0}^{n-1} \frac{[g_{ij}(x)]^k}{k!} \right\} p_i^{n-1}(1 - p_i) \end{aligned} \tag{4}$$

The expression in Equation (4) can be simplified in the following manner:

$$\begin{aligned} F_{ij}(x) &= (1 - p_i) \left\{ \sum_{n=1}^{\infty} p_i^{n-1} - \exp[-g_{ij}(x)] \sum_{n=1}^{\infty} \sum_{k=0}^{n-1} \frac{[g_{ij}(x)]^k}{k!} p_i^{n-1} \right\} \\ &= (1 - p_i) \left\{ \sum_{n=1}^{\infty} p_i^{n-1} - \exp[-g_{ij}(x)] \left(\sum_{n=1}^{\infty} p_i^{n-1} \right) \left(\sum_{k=0}^{\infty} \frac{[g_{ij}(x)]^k}{k!} p_i^k \right) \right\} \\ &= 1 - \exp[-g_{ij}(x)] \exp[p_i g_{ij}(x)] \end{aligned} \tag{5}$$

since

$$\sum_{n=1}^{\infty} p_i^{n-1} = \frac{1}{1 - p_i} \tag{6}$$

which gives

$$F_{ij}(x) = 1 - \exp[-(1 - p_i)g_{ij}(x)] \tag{7}$$

From Equation (7) it can be seen that the problem of determining the distribution function $F_{ij}(x)$ now reduces to that of estimating $g_{ij}(x)$, which can be determined from Equation (1) provided that $\lambda_{ij}(\xi)$ is known.

To estimate $\lambda_{ij}(\xi)$, it is necessary to establish the density of set j seed points, per unit length of OP, at distance r from OP, where r is measured along the set j fracture, and the probability that a fracture growing from one of the seed points intersects the fracture from set i.

First, let ρ_j be the density of fractures from set j. In general, ρ_j may be a function of location, but in this analysis it is assumed to take a homogeneous value. Consider the shaded parallelogram in Figure 3, which has unit length parallel to OP and width $\Delta r \sin\theta_{ij}$. Remembering that fractures from set j may originate on either side of OP, the required density is $2\rho_j \sin\theta_{ij}\Delta r$.

The probability, $\pi_{ji}(r)$, that an individual fracture from set j seeded at a distance r from OP intersects the fracture from set i, is given by

$$\pi_{ji}(r) = \begin{cases} 1 - F_{ji}(r) & t_{ji} < t_{ij} \\ 0 & \text{otherwise} \end{cases} \tag{8}$$

where t_{ij} is the time taken by the fracture from set i to reach the point of potential intersection with the fracture belonging to set j, and t_{ji} is the time taken by the fracture from set j to reach the same point.

To calculate the times to intersection, it is necessary to consider the velocities with which fractures propagate. Assuming that the velocities of propagation of fractures belonging to sets i and j, $u_i(x,t)$ and $u_j(x,t)$, respectively, are independent, and that they are a function only of time and distance of the growing tip from the seed point, the initial value problems

$$\frac{d}{dt}[x(t)] = u_i(x, t) \qquad x(t_0) = 0 \tag{9}$$

and

$$\frac{d}{dt}[r(t)] = u_j(r, t) \qquad r(t_0) = 0 \tag{10}$$

have to be solved to determine t_{ij} and t_{ji}. In principle, the analysis could be continued in greater generality. However since, it is assumed here that the velocities

of propagation, u_i and u_j, are constant for each fracture set, and that all fractures begin to grow simultaneously, $t_{ij} = \xi/u_i$ and $t_{ji} = r/u_j$.

In this case, $\pi_{ji}(r)$ is given by

$$\pi_{ji}(r) = \begin{cases} 1 - F_{ji}(r) & r < \dfrac{u_j}{u_i}\xi \\ 0 & \text{otherwise} \end{cases} \tag{11}$$

Hence an estimate of $\lambda_{ij}(\xi)$ is given by

$$\lambda_{ij}(\xi) = \int_0^{\frac{u_j}{u_i}\xi} 2\rho_j \sin\theta_{ij} \,[\,1 - F_{ji}(r)]\, dr \tag{12}$$

and so, from Equation (1)

$$g_{ij}(x) = \int_0^x \int_0^{\frac{u_j}{u_i}\xi} 2\rho_j \sin\theta_{ij}[1 - F_{ji}(r)]\, dr d\xi \tag{13}$$

From Equations (7) and (13) it can be seen that $F_{ij}(x)$ is a function of $F_{ji}(r)$:

$$F_{ij}(x) = 1 - \exp\left[-2(1 - p_i)\rho_j \sin\theta_{ij} \int_0^x \int_0^{\frac{u_j}{u_i}\xi} 1 - F_{ji}(r)\, dr d\xi\right] \tag{14}$$

Since the choice of set i is arbitrary, similar relationships can be written down which express $F_{ji}(r)$ as a function of $F_{ij}(x)$, namely,

$$F_{ji}(r) = 1 - \exp\left[-2(1 - p_j)\rho_i \sin\theta_{ij} \int_0^r \int_0^{\frac{u_i}{u_j}\zeta} 1 - F_{ij}(x)\, dx d\zeta\right] \tag{15}$$

Equations (14) and (15) can be combined to give the following closed form equation in $F_{ij}(x)$;

$$F_{ij}(x) = 1 - \exp\left[-2(1 - p_i)\rho_j \sin\theta_{ij} \int_0^x \int_0^{\frac{u_j}{u_i}\xi} \times \exp\left(-2(1 - p_j)\rho_i \sin\theta_{ij} \int_0^r \int_0^{\frac{u_i}{u_j}\zeta} 1 - F_{ij}(x)\, dx\, d\zeta\right) dr\, d\xi\right] \tag{16}$$

in which x is used as the dummy variable in the inner integral to emphasize the identity of the two occurrences of $F_{ij}(x)$ in the equation.

Multiple Fracture Sets

The above development deals only with the case of two fracture sets, but the analysis generalizes to the case of multiple fracture sets quite simply.

In the two fracture set case, $g_{ij}(x)$ is the expected number of encounters of the growing fracture from set i with preexisting fractures from set j. In the case of multiple fracture sets, define $g_i(x)$ to be the expected number of intersections along OP with preexisting fractures from sets other than set i. Clearly,

$$g_i(x) = \sum_{\substack{j=1 \\ j \neq i}}^{n} g_{ij}(x) \tag{17}$$

where n is the number of fracture sets, and the cdf, $F_i(x)$, is given by

$$F_i(x) = 1 - \exp[-(1 - p_i)g_i(x)] \tag{18}$$

In the case of multiple fractures sets, the probability that a fracture from set j intersects the growing fracture from set i, $\pi_{ji}(r)$, is given by

$$\pi_{ji}(r) = \begin{cases} 1 - F_j(r) & r < \dfrac{u_j}{u_i}\xi \\ 0 & \text{otherwise} \end{cases} \tag{19}$$

Hence, employing the same logic as in the two set case,

$$F_i(x) = 1 - \exp\left[-2(1 - p_i) \sum_{\substack{j=1 \\ j \neq i}}^{n} \int_0^x \int_0^{\frac{u_j}{u_i}\xi} \rho_j \, \sin\theta_{ij} [1 - F_j(r)] \, dr \, d\xi \right] \tag{20}$$

and similarly,

$$F_j(r) = 1 - \exp\left[-2(1 - p_j) \sum_{\substack{k=1 \\ k \neq j}}^{n} \rho_k \, \sin\theta_{jk} \int_0^r \int_0^{\frac{u_k}{u_j}\zeta} 1 - F_k(x) \, dx \, d\zeta \right] \tag{21}$$

The equation corresponding to Equation (16) for the case of two fracture sets thus becomes

$$F_i(x) = 1 - \exp\left[-2(1-p_i) \sum_{\substack{j=1 \\ j\neq i}}^{n} \rho_j \sin\theta_{ij} \int_0^x \int_0^{\frac{u_j}{u_i}\xi} \times \exp\left(-2(1-p_j) \sum_{\substack{k=1 \\ k\neq j}}^{n} \rho_k \sin\theta_{jk} \int_0^r \int_0^{\frac{u_k}{u_j}\zeta} 1 - F_k(x)\, dx\, d\zeta \right) dr\, d\xi \right] \tag{22}$$

APPROXIMATIONS TO $F_i(x)$

Equation (20) can be used as an iterative scheme for simultaneously calculating $F_i(x)$ for $i = 1, \ldots, n$. With this in mind, Equation (22) can be thought of merely as two sequential applications of Equation (20). However, by selecting suitably simple initial estimates of $F_k(x)$, Equation (22) can be used to demonstrate the development of analytical expressions representing lower and upper bounds to $F_i(x)$.

The selection of initial estimates of $F_k(x)$ can be achieved by considering again the case of a growing fracture from set i intercepted by fractures from set j. The fractures from set j may themselves be blocked by fractures from set k ($k \neq j$). Simple assumptions about the likelihood of this blocking lead to two extreme values of $F_i(x)$.

Lower Bound

Assume that all fractures from set k that are seeded close enough to a fracture from set j to intersect it have a probability of intersection of 1. That is, for each j, the initial estimate of $F_k(x)$ is given by

$$F_k(x) = \begin{cases} 0 & \text{for } x < \dfrac{u_k}{u_j} r \\ 1 & \text{otherwise} \end{cases} \tag{23}$$

This assumption produces fractures in set i that are too long, giving a lower bound for the cdf, $F_i^{\min}(x)$, since the fractures from set j that would naturally inhibit the growth of the original fracture from set i have their own growth blocked too frequently by fractures from set k.

Substituting the value for $F_k(x)$ given in Equation (23) into the right-hand side of Equation (22) and performing the two innermost integrations gives

$$F_i^{\min}(x) = 1 - \exp\left[-2(1-p_i)\sum_{\substack{j=1\\ j\neq i}}^{n} \rho_j \sin\theta_{ij} \int_0^x \int_0^{\frac{u_j}{u_i}\xi} \exp(-b_j r^2)\, dr\, d\xi\right] \tag{24}$$

where

$$b_j = (1-p_j)\sum_{\substack{k=1\\ k\neq j}}^{n} \rho_k \sin\theta_{jk} \frac{u_k}{u_j} \tag{25}$$

Performing the first of the remaining integrations in Equation (24) gives

$$F_i^{\min}(x) = 1 - \exp\left[-2(1-p_i)\sum_{\substack{j=1\\ j\neq i}}^{n} \rho_j \sin\theta_{ij} \int_0^x \frac{1}{2}\sqrt{\frac{\pi}{b_j}}\operatorname{erf}\left(\sqrt{b_j}\frac{u_j}{u_i}\xi\right) d\xi\right] \tag{26}$$

and completing the last integration gives the result:

$$F_i^{\min}(x) = 1 - \exp\left[-\sum_{\substack{j=1\\ j\neq i}}^{n} \frac{a_{ij}}{b_j}\left\{\sqrt{\pi b_j}x\operatorname{erf}\left(\sqrt{b_j}\frac{u_j}{u_i}x\right) + \frac{u_i}{u_j}\left[\exp\left(-\frac{b_j u_j^2}{u_i^2}x^2\right) - 1\right]\right\}\right] \tag{27}$$

where

$$a_{ij} = (1-p_i)\rho_j \sin\theta_{ij} \tag{28}$$

Upper Bound

An upper bound can be produced in a similar manner by assuming that no fractures from set k inhibit the growth of fractures from set j, and hence fractures from set i are foreshortened. This means that the initial value for $F_k(x)$ is given by

$$F_k(x) = 1 \quad \text{for all} \quad x \tag{29}$$

Substituting unity for $F_k(x)$ into the right-hand side of Equation (22) gives the upper bound of $F_i(x)$:

$$F_i^{\max}(x) = 1 - \exp\left[-2(1-p_i)\sum_{\substack{j=1\\ j\neq i}}^{n} \rho_j \sin\theta_{ij} \int_0^x \int_0^{\frac{u_j}{u_i}\xi} 1\, dr\, d\xi\right]$$

$$= 1 - \exp\left[-(1-p_i)\sum_{\substack{j=1\\ j\neq i}}^{n} \rho_j \sin\theta_{ij}\, \frac{u_j}{u_i} x^2\right] \tag{30}$$

and hence

$$F_i^{\max}(x) = 1 - \exp[-b_i x^2] \tag{31}$$

Full Iterative Approximation

The numerical, iterative approach using Equation (20) can be implemented using the simplest techniques. An example of the upper and lower bounds and the iterative approximation to the cdf for the case of three fracture sets, based upon parameter values in Table 2, is shown in Figure 4. It is interesting to note from the previous section that the lower bound is the result of a single application of Equation (20), using the upper bound as the initial estimate. A further application of Equation (20) leads to an approximation that is very close to the final one, and

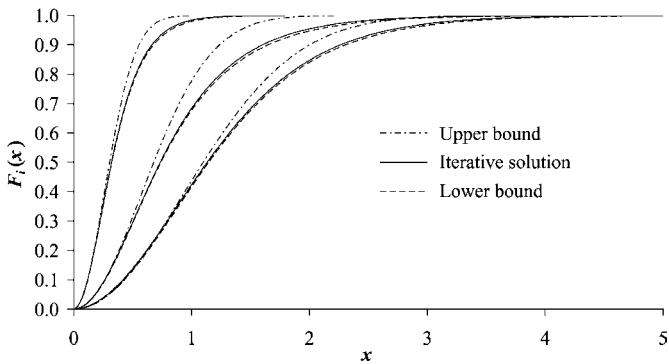

Figure 4. An example of the upper and lower bounds and the iterative approximation to cdf for a case with three fracture sets based upon the parameter set in Table 2.

hence the analytical expression for the lower bound is an efficient starting point for the numerical scheme. Since the scheme converges rapidly, it is conceivable that the lower bound might also be used as a rough approximation to the solution requiring no numerical techniques at all.

VERIFICATION OF THE MATHEMATICAL ANALYSIS

Since only approximations to $F_i(x)$ have been derived, numerical experiments have been conducted to assess their accuracy. In each simulation, fracture patterns were generated on a rectangular domain using a computer code, FGEN, and the empirical distribution of X_i calculated. Where generated fractures were censored by the edge of the generation domain, the censored part of the fracture was not included in the length statistics. Other edge effects were minimized simply by employing a large domain relative to the density of fracturing and typical maximum fracture trace length. Comparisons between the empirical cdf of X_i derived from simulation results and the analytical approximation are generally good (Fig. 5). Model parameter values for the simulations in Figure 5 are given in Tables 1 and 2.

DISTRIBUTION OF FRACTURE TRACE LENGTHS

The probability density function of the full fracture trace length can be calculated from the numerical approximation. A Monte Carlo approach in which adding random samples from tabulated values of $F_i(x)$ in pairs is computationally inexpensive and provides a sufficiently robust approximation to the semianalytical fracture trace length pdf to enable the comparison between model results and the empirical trace length pdf to be made.

FRACTURE SPACING

The above analysis can be adapted to characterize the fracture spacing produced by the parallel fracture model in the following manner. For a given fracture set, i, generate a large set of points over the fractured area using a uniform Poisson process. Select one of the two directions orthogonal to the direction of the fracture set and, for each point, measure the shortest distance to a fracture from the same set in that direction. Then $S_i(x)$, the cdf of the measured distances, characterizes the fracture spacing of set i.

The form of $S_i(x)$ can be determined by considering a phantom fracture growing at right angles to the direction of set i from an arbitrary location with the properties that it does not impede the growth of any other fracture and that it stops when it meets the first fracture from set i. Then $S_i(x)$ is just the cdf of the length of all such phantom fractures.

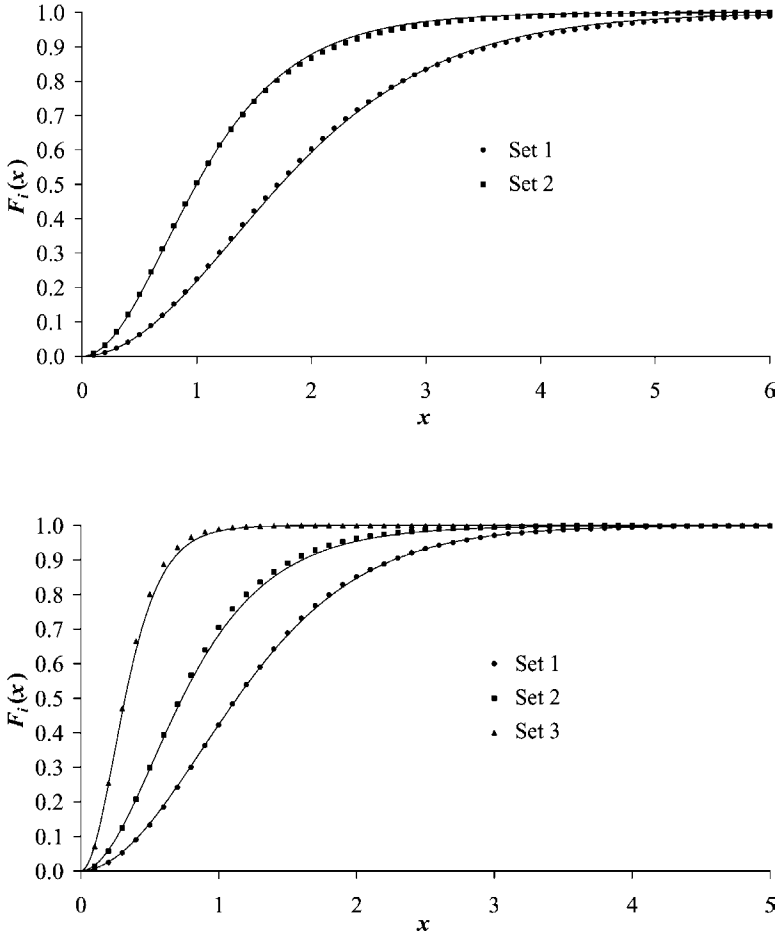

Figure 5. Comparisons between the empirical cdf of X_i derived from simulation results and the analytical approximation. Parameter values for (A) are given in Table 1 and for (B) in Table 2.

Table 1. Parameter Values Used for Figure 5(A)

Set	ρ	θ	u	p
1	1	90°	2	0
2	1	60°	1	0.2

Table 2. Parameter Values Used for Figure 5(B)

Set	ρ	θ	u	p
1	1	90°	2	0.2
2	2	60°	1	0
3	1	150°	0.5	0

The probability that an individual fracture from set i seeded at a distance r from the line of the phantom fracture intersects it is just $1 - F_i(r)$, and, following the logic behind Equation (12), the density of intersections with the phantom fracture is therefore the integral of twice the product of the density of seed points of set i and $1 - F_i(r)$, since $\theta = \pi/2$. That is,

$$\lambda_{ki}(x) = \int_0^\infty 2\rho_i[1 - F_i(r)]\,dr \tag{32}$$

where the subscript k indicates the phantom fracture and x its length.
The mean number of intersections with the phantom fracture is therefore

$$\begin{aligned} g_{ki}(x) &= \int_0^x \int_0^\infty 2\rho_i[1 - F_i(r)]\,dr\,d\xi \\ &= \alpha_i x \end{aligned} \tag{33}$$

where

$$\alpha_i = 2\rho_i \int_0^\infty [1 - F_i(r)]\,dr \tag{34}$$

and so

$$S_i(x) = 1 - \exp[-\alpha_i x] \tag{35}$$

which is an exponential distribution with mean $1/\alpha_i$.

DISCUSSION

The Form of the pdf of Fracture Trace Lengths

The pdf of the total fracture trace length produced by the growth algorithm has a zero derivative at the origin. This is because the total fracture length is

obtained by adding two independent samples from the part fracture trace length distribution. Theorem 1 shows that if $f_T(x)$ is an analytic pdf of the total trace length then $f'_T(0) = [f(0)]^2$, where $f(x)$ is the pdf of the part trace length. It can be determined from Equation (22) that $f(0) = 0$, and so it follows that $f'_T(0) = 0$.

THEOREM 1. Let $F_T(x)$ and $f_T(x)$ be the cumulative distribution function and the probability density function of the total trace length of fractures in a given set. Let $F(x)$ and $f(x)$ be the corresponding functions for the part trace lengths such that $F(0) = 0$ and $F^{(n)}(0)$ exists for all positive integers, n. Then $f'_T(0) = [f(0)]^2$.

Proof: The total trace length is determined by adding two independent samples from $F(x)$, and so

$$\begin{aligned} F_T(x) &= \int_0^x \int_0^{x-y} f(y) f(z)\, dz\, dy \\ &= \int_0^x f(y) F(x-y)\, dy \end{aligned} \tag{36}$$

since $F(0) = 0$.
Expanding $F(x - y)$ as a Taylor series about x gives

$$\begin{aligned} F_T(x) &= \int_0^x f(y) \sum_{n=0}^{\infty} (-1)^n \frac{y^n}{n!} F^{(n)}(x)\, dy \\ &= \sum_{n=0}^{\infty} (-1)^n F^{(n)}(x) \int_0^x \frac{y^n}{n!} f(y)\, dy \end{aligned} \tag{37}$$

The pdf, $f_T(x)$, is the derivative of $F_T(x)$ with respect to x, and so

$$f_T(x) = \sum_{n=1}^{\infty} (-1)^n \left\{ F^{(n+1)}(x) \int_0^x \frac{y^n}{n!} f(y)\, dy + F^{(n)}(x) \frac{x^n}{n!} f(x) \right\} \tag{38}$$

Differentiating gives

$$\begin{aligned} f'_T(x) = {} & F''(x) \int_0^x f(y)\, dy + 2F'(x) f(x) + F(x) f'(x) \\ & + \sum_{n=1}^{\infty} (-1)^n \left\{ F^{(n+2)}(x) \int_0^x \frac{y^n}{n!} f(y)\, dy + 2F^{(n+1)}(x) \frac{x^n}{n!} f(x) \right. \\ & \left. + F^{(n)}(x) \left[\frac{x^n}{n!} f'(x) + \frac{x^{n-1}}{(n-1)!} f(x) \right] \right\} \end{aligned} \tag{39}$$

from which

$$f'_{\mathrm{T}}(0) = [f(0)]^2 \tag{40}$$

since $F(0) = 0$. □

Comment

The production of only a small number of short fractures by this method, as indicated by the zero derivate of $f_{\mathrm{T}}(x)$ at the origin, can be understood physically by considering slow-growing fractures. Intuitively, the slow-growing fractures are expected on average to be short since they are likely to encounter more pre-existing fractures as they grow and have a greater chance of being terminated early on. However, at least one end of a slow-growing fracture can quickly become shielded from such encounters by those fractures that grow faster, at which point the slow speed of propagation becomes irrelevant to the fracture length and the fracture is allowed to grow, no matter how long it takes, until it encounters one of the shielding fractures. This results in the production of fewer very short fractures and a larger number of intermediate-length fractures in the set.

Further Development

The derivation of the distributions of part trace length, X_i, and semi spacing, S_i, is based upon the assumption that the fracture seed point locations can be described by a uniform Poisson process. This assumption also implies that X_i and S_i are the same for the two directions of fracture growth, and hence that the distributions of full fracture trace length and spacing can be derived by adding two independent samples of X_i and S_i, respectively. Together with Theorem 1, this implies that the cdf of full fracture trace lengths has a zero derivative at the origin, and that the cdf of the spacing has a positive derivative of α_i at the origin. Thus, the form of the method analyzed in this paper may not simulate well fracture systems that do not comply with these restrictions. In particular, the regular spacing seen in some fracture patterns can often be described by Weibull distributions, which have a zero derivative at the origin, reflecting a rarity of long, closely spaced parallel fractures. In contrast, Figure 2 shows a number of such fracture pairs. The numerical implementation of the growth algorithm can be modified quite simply to incorporate regular fracture spacing by introducing repulsion between seed points. However, the mathematical analysis of such a modified method is more difficult since the Poisson process assumption is violated. Further work is required on this issue.

SUMMARY

A class of statistically based fracture generation algorithms, based loosely upon the propagation of fractures, has been described. The base case algorithm, in which all fractures are initiated simultaneously, and in which fractures within a set are parallel, uniformly distributed in space, and grow at a constant speed, has been described. An analysis of the fracture trace lengths produced by this algorithm has been presented and assessed. An analysis of a measure of the fracture spacing produced by the algorithm has also been presented. The mathematical approximation of the base case model produces fracture trace length distributions with zero derivatives at the origin due to the two-directional growth and the assumption that this growth is independent of seed point location. Although the mathematical analysis is restricted to sets of parallel fractures, it could be applied heuristically to more complicated systems by subdividing fracture sets into subsets of parallel fractures.

A computer code, FGEN, has been developed to implement the algorithms and is available from the author.

ACKNOWLEDGMENTS

This research has been partly sponsored under the "Pollutant Transport in Soils and Rocks" special topic funded jointly by the Biotechnology and Biological Science Research Council (formerly the Agricultural and Food Research Council), and the Natural Environment Research Council, and represents part of a joint investigation undertaken by the Hydrogeology Research Group of the School of Geography, Earth and Environmental Sciences at University of Birmingham, the Fluid Processes Group of the British Geological Survey, and the Water Resource Systems Research Laboratory of the University of Newcastle upon Tyne.

REFERENCES

Gringarten, G., 1998, Fracnet: Stochastic simulation of fractures in layered systems: Comput. Geosci., v. 24, no. 8, p. 729–736.

Horgan, G. W., and Young, I. M., 2000, An empirical stochastic model for the geometry of two-dimensional crack growth in soil (with Discussion): Geoderma, v. 96, p. 263–289.

Josnin, J.-Y., Jourde, H., Fénart, P., and Bidaux, P., 2002, A three-dimensional model to simulate joint networks in layered rocks: Can. J. Earth Sci., v. 39, p. 1443–1455.

Lloyd, J. W., Greswell, R., Williams, G. M., Ward, R. S., Mackay, R., and Riley, M. S., 1996, An integrated study of controls on solute transport in the Lincolnshire Limestone: Q. J. Eng. Geol., v. 29, no. 4, p. 321–339.

Olsen, J. E., 1993, Joint pattern development: Effects of subcritical crack growth and mechanical crack interaction: J. Geophys. Res., v. 98, no. B7, p. 12251–12265.

Renshaw, C. E., and Pollard, D. D., 1994, Numerical simulation of fracture set formation: A fracture mechanics model consistent with experimental observations: J. Geophys. Res., v. 99, no. B5, p. 9359–9372.

Riley, M. S., Ward, R. S., and Greswell, R. B., 2001, Converging flow tracer tests in fissured limestone: Q. J. Eng. Geol. Hydrogeol., v. 34, no. 3, p. 283–297.

Swaby, P. A., and Rawnsley, K. D., 1996, An interactive 3D fracture modelling environment: Society of Petroleum Engineers, Tulsa, SPE 36004, Dallas, Texas, p. 177–187.